MICROCOPY RESOLUTION TEST CHART
NATIONAL BUREAU OF STANDARDS-1963-A

LEVEL

CONVECTIVE IGNITION
OF NITROCELLULOSE BASED PROPELLANTS
IN UNSTEADY FLOW FIELDS

July 1, 1978 to June 30, 1979

by

L. H. Caveny, A. Birk and W. A. Sirignano

Final Report to

July 1979

Transmitted by:

Leonard H. Caveny

Leonard H. Caveny
Co-Principal Investigator

Department of Mechanical & Aerospace Engineering
PRINCETON UNIVERSITY
Princeton, New Jersey

79 09 4 125

The findings in this report are not to be construed as an official Department of the Army position, unless so designated by other authorized documents.

SECURITY CLASSIFICATION OF THIS PAGE (When Data Entered)

REPORT DOCUMENTATION PAGE		READ INSTRUCTIONS BEFORE COMPLETING FORM
1. REPORT NUMBER	2. GOVT ACCESSION NO.	3. RECIPIENT'S CATALOG NUMBER MAE Report No. 1445
4. TITLE (and Subtitle) Convective Ignition of Nitrocellulose Based Propellants in Unsteady Flow Fields.		5. TYPE OF REPORT & PERIOD COVERED Final rept. 1 Jul 78- 30 Jun 79.
		6. PERFORMING ORG. REPORT NUMBER
7. AUTHOR(s) L. H./Caveny, A. Birk W. A. Sirignano		8. CONTRACT OR GRANT NUMBER(s) DAAG29-78-G-0153
9. PERFORMING ORGANIZATION NAME AND ADDRESS Department of Mechanical & Aerospace Engineering Princeton University Princeton, New Jersey 08544		10. PROGRAM ELEMENT, PROJECT, TASK AREA & WORK UNIT NUMBERS
11. CONTROLLING OFFICE NAME AND ADDRESS U. S. Army Research Office Post Office Box 1221 Research Triangle Park, NC 27709		12. REPORT DATE July 1979
		13. NUMBER OF PAGES 20
14. MONITORING AGENCY NAME & ADDRESS(If different from Controlling Office) MAE-1445		15. SECURITY CLASS. (of this report) Unclassified
		15a. DECLASSIFICATION/DOWNGRADING SCHEDULE NA

16. DISTRIBUTION STATEMENT (of this Report)

Approved for public release; distribution unlimited.

17. DISTRIBUTION STATEMENT (of the abstract entered in Block 20, if different from Report)

NA

18. SUPPLEMENTARY NOTES

The findings in this report are not to be construed as an official Department of the Army position, unless so designated by other authorized documents.

19. KEY WORDS (Continue on reverse side if necessary and identify by block number)

Solid Propellant Ignition   Nonsteady Combustion
Convective Ignition   Double Base Propellant
Cylinders in Crossflow
Unsteady Heat Transfer

20. ABSTRACT (Continue on reverse side if necessary and identify by block number)

This is a report on a continuing research directed at convective ignition of nitrocellulose-based propellants. The research encompasses flame theory, chemistry, and fluid dynamics. The primary objectives of the research are to determine the site and mode of convective ignition of propellant cylinders in crossflow and to determine the influence of igniter gas composition on the ignition events. Work is well under way to determine the conditions for which ignition occurs at the leading edge, in the separation zone or in the wake. (continued on reverse side)

DD FORM 1473 EDITION OF 1 NOV 65 IS OBSOLETE   UNCLASSIFIED
1 JAN 73

SECURITY CLASSIFICATION OF THIS PAGE (When Data Entered)

20. ABSTRACT (continued...)

The laboratory approach developed (i.e., the use of a shock tunnel as the convective heating device) has been proved successful and over one hundred shock tunnel experiments have been conducted. All diagnostic devices (such as thin film gauges, miniature pressure transducer and radiation detectors) proposed last year were designed, fabricated and used successfully. Attention was focused on the different behavior of single, double and triple based propellants under the same test conditions, and on the importance of the transient boundary layer development time on ignition trends. To validate and substantiate the ignition trends, additional data collection and development of analytical models are needed.

TABLE OF CONTENTS

Accession For

NTIS GRA&I

DDC TAB

Unannounced

Justification

By

Distribution/

Availability Codes

Dist | Avail and/or
special

A

PREFACE

INTRODUCTION

This is a report on continuing research directed at the convective ignition of nitrocellulose-based propallants. Interpretations of the experiments have indicated three main mechanisms of ignition; i.e., ignition occurs at the (1) leading edge, (2) trailing edge, or (3) around the separation point. A full discussion of these mechanisms is given in the chapter on analytical approach. It has been found that double-based propellants (M-26) are much more sensitive to oxidizers in the convective flow than the triple-based propellant (M-30). The present phase of the research will be described next, followed by a technical approach for the continuing effort.

PRESENT WORK

During the first stage of the present phase of the research program, all equipment and instrumentation tasks were completed and satisfactory operation of the system was verified by preliminary tests. Operation of the shock tunnel was extended to the range of desired Reynolds number by the use of a special adjustable choking nozzle downstream of the test section. A new technique for ignition detection which offers high spatial resolution was tried successfully. A line scanning array detector (i.e., camera) was used to detect ignition of the cylindrical propellant with a spatial resolution of 5 degrees of cylinder perimeter and time resolution of 0.2 msec. An array of 64 light-sensitive elements serves as the detector. For the fast ignition conditions, the present detector used is marginal in light sensitivity capabilities (especially in the near-ultraviolet spectrum used for detection to avoid background noise) and time resolution. However the ignition behavior on the entire propellant surface can be observed simultaneously. High speed motion pictures of ignition propellants with aluminum tracers were taken to observe the flow features in the wake. The burning aluminum particles serving as tracers revealed the flow patterns. Layout of instrumentation is given in Figure 1. During the second stage of the present work, tests were conducted regularly with different propellants, mainly M-26 and M-30. Some heat flux data were collected and the analytical development aimed at interpretation of the experimental observations was started.

Though the number of experiments conducted is far from being sufficient to characterize the ignition trends of each propellant,

an overall ignition performance envelope started to take form. The nominal test conditions were: temperature 1800-1900 K, pressure,1.3 to 2 MPa; velocity, 0-100 m/sec; gas composition; 0 to 50% oxygen in nitrogen. The primary observations are:

A) No ignition occurred above Reynolds number of about 60,000 for any propellant when the flow contained less than 50% oxygen.

B) No ignition was obtained for M-1 and M-26 under fully inert flow (0% oxygen) even for free stream temperatures as high as 2500 K.

C) When even a small amount of oxygen (2%) was present in the flow, ignition occurred very rapidly for M-26 and ignition delay times of sub-millisecond were measured for flows containing higher contents of oxygen. This range of time is close to the relaxation time of the boundary layer. Hence, the analyses of the transient development of the boundary layer flow coupled with the heat up of the solid phase and the gas phase chemical reactions leading to ignition are important.

D) Heat flux measurements using the special heat flux gauge developed for this purpose revealed very high heat fluxes resulting in steep rise of surface temperature during the very first stages of the flow around the cylinder. The rapid increase in surface temperature may lead to very rapid ignition under favorable conditions, such as the oxidizers present in the igniter combustion products.

E) As mentioned previously, three main regions of ignition were clearly observed using the radiation detectors and high speed photography.

To summarize the data collected, several figures are given here. Figures 2 and 3 present a set of thin film gauge data. Figure 4 is a plot of ignition delay times for M-30 under the nominal test conditions. M-30 was the only propellant for which ignition was detected for inert flow (i.e., 100% N2). Flame spreading trends for M-30 are shown in Figure 5. Figure 6 is a summary of ignition occurrences for several types of propellants in the Reynolds numbers range covered in the experiments.

Figure 7 is an example of a high-speed motion picture sequence of propellant igniting. Within 0.25 ms of the onset of convective heating, vapors originating at the front surface have been ignited and are burning. During the transients to full flame development, the vapors burn out and are then re-established permanently within the next 0.5 ms. After 1.5 ms, the combined effects of convective heating and heat feeedback from the propellant decomposition produce sustained combustion over the entire surface of the cylinder.

ANALYTICAL MODEL TO BE DEVELOPED DURING RENEWAL EFFORT

INTRODUCTION

Three main regions of ignition have been distinguished during the experimental work conducted. They will be referred to as:

(a) Front stagnation region ignition

(b) Separation region ignition

(c) Rear body ignition

See illustrations in Fig. 8.

The occurrence of the first event (a) is independent of the flow in regions (b) and (c), but events (b) and (c) are interrelated and depend on the flow in region (a). Favored occurrence of any of those events depends on the following factors: (1) Content of oxidizer in free stream; (2) Reynolds number of the flow; (3) Gas phase and surface Damkohler numbers; (4) Ratio of thermal and diffusional properties of gaseous phase and solid phase.

Based on our experimental results (see Fig. 5), event (a) will be favored in cases of high free stream oxidizer and long flow residence time (namely, low Reynolds number). In fact, some ignition events occurred in a time scale which was within the relaxation time of boundary layer formation around the front half of the cylinder.

Unlike convective ignition of liquid spray droplets which may be considered to occur in a quasi-steady gas phase (1), the ignition of solid propellant cylinder may occur in the transient gas phase. While both types of convective ignition may occur in the same range of external flow velocities, the residence-time of flow around the droplets is orders of magnitude shorter than that of flow around the propellant cylinders (considered in this study) due to the much smaller size of the droplets (order of 100 micron). The higher than atmospheric pressure associated with solid propellant ignition results in lower ratios of gas and solid phases diffusivities. Since Damkohler numbers and diffusivities ratios are dominant factors in determining ignition events, the overall conclusion is that transient development of gaseous phase should not be overlooked when analyzing ignition behavior of cylindrical solid propellants.

While a complete set of equations to describe the flow at regions (b) and (c) is unavailable at this point due to the complexity of flow and uncertainty of length scales in these regions, the equations of front stagnation flow reacting boundary layers can be written in a manner suitable for numerical solution. Since these equations include the transient behavior of the gaseous phase and all families of parameters pertinent to ignition events, solution of those equations will elucidate the mechanism of ignition in regions (b) and (c) as well. Therefore it is proposed that the analytical work should take three directions:

1) Numerical solution of front stagnation point equations. (Region a)

2) Phenomelogical approach to treat ignition in regions (b) and (c). It may contain solution of simplified equations.

3) Overall parametric grouping of ignition delay times.

Work is now in progress on the numerical solution of equations for region (a) as described in the next section.

A subsequent section deals with possible mechanisms of ignition in regions (b) and (c). Features of the flow in regions (b) and (c) are supported by the experimental results, mainly: a) Heat flux measurements; b) High speed shadowgraph photography of flow including Aluminum tracers; c) Variations of half-inert, half-propellant test samples.

Front Stagnation Flow Equations

Assumptions

1. Prandtl, Schmidt and Lewis numbers equal to unity.
2. Same physical properties to all gaseous species.
3. One step irreversible global chemical reaction in the gaseous phase subjected to second order Arrhenius kinetics.

    $[F] + n[OX] \rightarrow (n+1)[P]$
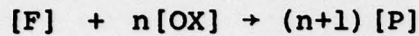
4. Solid phase decomposition is endothermic and is subjected to Arrhenius pyrolysis law. The solid is decomposed as following.

    $[Solid] \rightarrow \alpha[F] + (1-\alpha)[OX]$
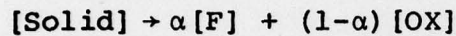
5. At time $t = 0$, the propellant is suddenly immersed in a flow field characterized by velocity V_∞, temperature T_∞, pressure P_∞ and oxidizer content $Y_{OX\infty}$.

Gas Phase Chemical Reaction:

$$\frac{dY_F \rho}{dt} = \frac{1}{n} \frac{dY_{OX} \rho}{dt} = -\rho^2 A_R Y_F Y_{OX} e^{-E_R/RT}$$

Solid Phase Decomposition:

$$V_{\rho 0} = A_p e^{-E_p/RT} {}_w \qquad \text{(Solid regression velocity)}$$

Using similarity variables $\eta = \dfrac{\displaystyle\int_0^\infty \rho \, dy}{\sqrt{\rho_e \mu_e t_f}}$ for the gaseous phase,

$\eta_s = \sqrt{\dfrac{\rho_{so} C_{pso}}{t_f K_{so}}}\, y$ for the solid phase and nondimensional time

$\tau = t/t_f$ where $t_f = \dfrac{R}{2U_\infty}$ is the characteristic residence time of

flow in front stagnation region, the following set of equations is obtained.

$$- \frac{\partial G}{\partial \tau} + \frac{\partial^2 G}{\partial \eta^2} + F \frac{\partial G}{\partial \eta} = G^2 - \theta \tag{1}$$

$$\frac{\partial F}{\partial \eta} = G \tag{2}$$

$$- \frac{\partial Z}{\partial \tau} + \frac{\partial^2 Z}{\partial \eta^2} + F \frac{\partial Z}{\partial \eta} = 0 \tag{3}$$

$$- \frac{\partial H}{\partial \tau} + \frac{\partial^2 H}{\partial \eta^2} + F \frac{\partial H}{\partial \eta} = 0 \tag{4}$$

$$- \frac{\partial Y_I}{\partial \tau} + \frac{\partial^2 Y_I}{\partial \eta^2} + F \frac{\partial Y_I}{\partial \eta} = 0 \tag{5}$$

$$- \frac{\partial \theta}{\partial \tau} + \frac{\partial^2 \theta}{\partial \eta^2} + F \frac{\partial \theta}{\partial \eta} = - \left[(H - \theta) \frac{\eta}{h} + Z \right] \left[\frac{H - \theta}{\theta} \right] D_G e^{-\theta R / \theta} \tag{6}$$

$$- \frac{\partial \theta_{so}}{\partial \tau} - \left(\frac{D_s}{\epsilon} \right)^{\frac{1}{2}} \cdot \gamma \cdot e^{-\theta_p / \theta_w} \frac{\partial \theta_{so}}{\partial \eta_{so}} + \frac{\partial^2 \theta_{so}}{\partial \eta^2_{so}} = 0 \tag{7}$$

Boundary conditions

At time $\tau = 0$, for any η and $\eta_{so} > 0$ (8)

    $G = 1$ (a)

    $\theta = 1$ (b)

    $Z = Y_{OXe}$ - given   (c)

    $H = 1 + \frac{h}{n} Y_{OXe}$ (d)

    $Y_I = 1 - Y_{OXe}$ (e)

    $\theta_{so} = \theta_{so}(\tau=0)$ - given   (f)

At $\eta = \eta_{so} = 0$ for any τ.   (9)

    $G_w = 0$ (a)

    $F_w = - (D_s)^{\frac{1}{2}} e^{-\theta_p / \theta_w}$ (b)

    $\left(\frac{\partial Z}{\partial \eta} \right)_w + F_w Z_w = [1 - \alpha(1+n)] F_w$ (c)

$$\left(\frac{\partial H}{\partial \eta}\right)_w + F_w H_w = \left(\frac{\partial \theta}{\partial \eta}\right)_w + F_w[\theta_w + (1-\alpha)\frac{h}{n}]$$

(d)

$$\left(\frac{\partial Y_I}{\partial \eta}\right)_w + F_w Y_{Iw} = 0$$

(e)

$$-\left(\frac{\partial \theta}{\partial \eta}\right)_w - (\varepsilon)^{\frac{1}{2}}\left(\frac{\partial \theta_{so}}{\partial \eta_{so}}\right)_w = F_w g$$

(f)

At $\eta = \eta_{so} = \infty$ for any τ.   (10)

$G_\infty = 1$ (a)

$\theta_\infty = 1$ (b)

$Z = Y_{OXe}$ - given   (c)

$H = 1 + \frac{h}{n} Y_{OXe}$ (d)

$Y_I = 1 - Y_{OXe}$ (e)

$\theta_{so} = \theta_{so\infty}$ - given   (f)

where:

F - stream function so that $u = \frac{2u_\infty x}{R}\frac{\partial F}{\partial \eta}$

$Z \triangleq Y_{OX} - nY_F$

OX - Oxidizer	e - edge of boundary
F - Fuel	layer
I - Inert	∞ - infinity
So - Solid	w - wall

$H \triangleq \theta + \frac{h}{n} Y_{OX}$

$\theta \triangleq \frac{T}{T_e}$ nondimensional gas phase temperature.

$\theta_{so} \triangleq \frac{T_{so}}{T_e}$ nondimensional solid phase temperature.

$D_G = A_R \rho_e t_f$ - Gas phase Damkohler number. Ratio of residence time to reaction time.

$$D_s = \frac{\rho_{so}^2 A_p^2 t_f}{\rho_e \mu_e}$$

   – Surface Damkohler number. Ratio of residence time to fuel loading time.

$$\varepsilon = \frac{\rho_{so} K_{so} C_{pso}}{\rho_e K_e C_{pe}}$$

   – Thermal properties ratio of solid phase to gas phase. A measure of thermal response of solid phase to changes in gas phase.

$$\gamma = \frac{C_{pso}}{C_{pe}}$$

   – Heat capacity ratio.

$$h = \frac{Q}{C_{pe} T_e}$$

   – Ratio of heat of reaction to static enthalpy of flow.

$$g = \frac{L_v}{C_{pe} T_e}$$

   – Ratio of heat of evaporation to static enthalpy of flow.

$$\theta_R = \frac{E_R}{RT_e}$$

   – Nondimensional activation energy of reaction.

$$\theta_p = \frac{E_p}{RT_e}$$

   – Nondimensional pyrolysis activation energy.

Ignition Criteria

Following Ref. (2), two ignition criteria will be employed. The first one considers ignition to occur when some bulge in boundary layer temperature profile occurs. Thus

$\theta(t_{ign}) > a \theta_e$ where a may be taken arbitrarily as 1.5.

The second criterion considers ignition to occur when steep rise in light intensity (I) emitted from products species is detectable. The second criterion is more suitable to interpretation of ignition tests.

$$I \simeq A \int_0^\infty Y_P \, e^{-\frac{E_L}{\theta}} \, d\eta$$

A and E_L some constants.

$$Y_P = 1 - Y_F - Y_{OX} - Y_I$$

Thus ignition occurs when:

$$\frac{dI}{d\tau} = \frac{d}{d\tau} \left(A \int_0^\infty (1 - Y_F - Y_{OX} - Y_I) e^{-\frac{E_L}{\theta}} \, d\eta \right) > b$$

b may be chosen arbitrarily.

Features of Ignition in Stagnation Flow

The external flow around the front half of a cylinder satisfies (up to about 60 degrees). $U_e = 2 U_\infty \sin \frac{X}{R}$ which may be written as:

$$U_e = 2 U_\infty \left(\frac{X}{R} - \frac{1}{3!} \left(\frac{X}{R} \right)^3 + \frac{1}{5!} \left(\frac{X}{R} \right)^5 - \ldots \right).$$

Stagnation flow is the region where $U_e = 2 U \frac{X}{R}$ is very closely satisfied which extends about 30 degrees from front stagnation point on the cylinder perimeter. That region is characterized by having constant (approximately) boundary layer thickness and unchanging profiles of velocity, temperature and species concentration along the x-coordinate. Therefore there is not any preference for ignition event to occur at any specific x in this region. Furthermore, surface temperature is constant with x and the accumulated amount of fuel evaporated along x is balanced exactly by dilution from the external flow so that reaction rate is the same everywhere and ignition if it occurs should occur simultaneously over the entire region which subtends about 60 degrees of the cylinder perimeter.

Under some conditions, ignition may occur during the transient development of the boundary layer. In this case, significant solid phase decomposition reaction rate in the gaseous phase occurs when the boundary layer is still very thin. The bootstrapping process of

heat feedback to the surface is very intense then, due to the proximity of the reaction zone to the surface and onset of ignition may occur abruptly.

Ignition Mechanism in Regions (b) and (c)

General Features of the Flow Beyond the Front Stagnation Region

As the flow leaves the front stagnation region, the rate of external flow velocity acceleration ($\frac{\partial u_e}{\partial x}$) decreases, and the boundary layer thickens until separation of flow occurs at around 90 degrees where $(\frac{\partial u}{\partial y})_w = 0$. The equations describing this flow are three dimensional in x, η and τ and therefore are an order of magnitude more difficult to solve than the front stagnation region equations. They will not be given here.

The fluid in the wake flows from the rear stagnation point to the separation points with periodic fluctuation of about $0.2 \cdot \frac{U_\infty}{2R} = \frac{0.05}{t_f}$ which is the frequency of vortex shedding in the wake. The circulation velocity in the wake U_w depends on the Re number and it is in the range of $\sim 0.5\ U_\infty$ [see (5)]. No simpler equation than the Navier Stokes themselves can be written to describe the flow in this region. Thus any attempt to predict ignition in regions (b) and (c) will be phenomenological in essence, taking into account the general features of flow in these regions (which are observed experimentally).

Rear Body Ignition [Region (C)]

The basic principles behind the suggested analytic treatment are given by (3) and (4) which treat heat transfer to the rear base of a cylinder or a bluff body. The same rationale is extended to the treatment of ignition mechanism of propellant in this region.

The basic mechanism is that of renewed wake vortex flow at a frequency $f = \frac{0.05}{t_f}$ (the vortex shedding frequency). Every time as a new vortex is established, the rear portion of the cylinder is suddenly exposed to a flow of velocity U_w temperature T_∞ and

oxidizer content $Y_{OX\infty}$. The surface temperature of the propellant T_w rises with time as every cycle contributes heat flux to the surface. During each cycle, the flow around the rear stagnation point can be described similarly to the front stagnation point equations starting every time from new higher solid phase temperature distribution. The significance of the transient time of boundary layer development on the rear surface depends on the ratio of the wake flow residence time $t_w \simeq \frac{R}{2U_w}$ to the cycle time $T \simeq 10 \frac{R}{U_\infty}$. If $\frac{t_w}{T} \simeq \frac{U_\infty}{20\,U_w} > 0.5$, the flow is mainly transient. Heat flux during the transient time is higher than that during the steady state. Since the transient time is at least 10% of the period time, the transient features of ignition must be taken into account.

Note that in front stagnation flow (in cases when ignition times are much longer than the transient time of boundary layer relaxation), the time dependence of the boundary layer equations may be omitted, thus treating the gaseous phase as quasi-steady and not transient. The rear stagnation point cannot be treated this way because of the cyclic renewal of flow. Though rear surface temperature generally lags that of the front stagnation region surface which means lower decomposition rates, the sudden proximity of gas phase reaction zone to the surface at the outset of any new cycle means instantaneously high heat flux feedback to the solid phase and possible ignition.

Separation Region Ignition

Though it is difficult to assign any length scales to this region, it will be referred to as the region confined between the separation line and the propellant wall in close proximity to the separation point which is around 90 degrees. It is assumed that the residence time of any fluid lump in this region is much longer than t_f or t_w. Since the gas temperature on the separation line is that of the bottom portion of the separated boundary layers (which is close to T_{ws}), it is assumed that the gas temperature in this region is about T_{ws}. Species concentrations in this region

accumulate by diffusion and convection to values which are close to the highest corresponding values on the boundaries. Thus Y_{FS} = the highest of Y_{FB} or Y_{FW} (generally Y_{FB}). The same with Y_{OXs}. Experimentally it has been found that T_{WS} is the slowest growing surface temperature. Ignition occurs when the rate of temperature growth in the gaseous phase due to possible chemical reaction between the fuel and oxidizer is much higher than the rate of temperature growth of the propellant surface, T_{WS} is

$$\frac{d}{dt}\left[\frac{Q\rho^2 A_R}{C_p}\, Y_{OXs}\, Y_{FS}\, e^{-\frac{E_R}{RT_{WS}}}\right] >> \frac{d}{dt}\,[T_{Ws}]$$

$\frac{d}{dt}\,[T_{Ws}]$ is calculated using empirical heat flux relations. Y_{FS} and Y_{OXs} may be approximated by calculating the amount of dilution of solid phase decomposition gases of the front half with the external flow in the boundary layer.

Ignition may be favored in this region because of the absence of convective flow to sweep the reacting species off the surface or, in other words, very long residence times. Postponement of ignition is due to the slow growth of T_{Ws}.
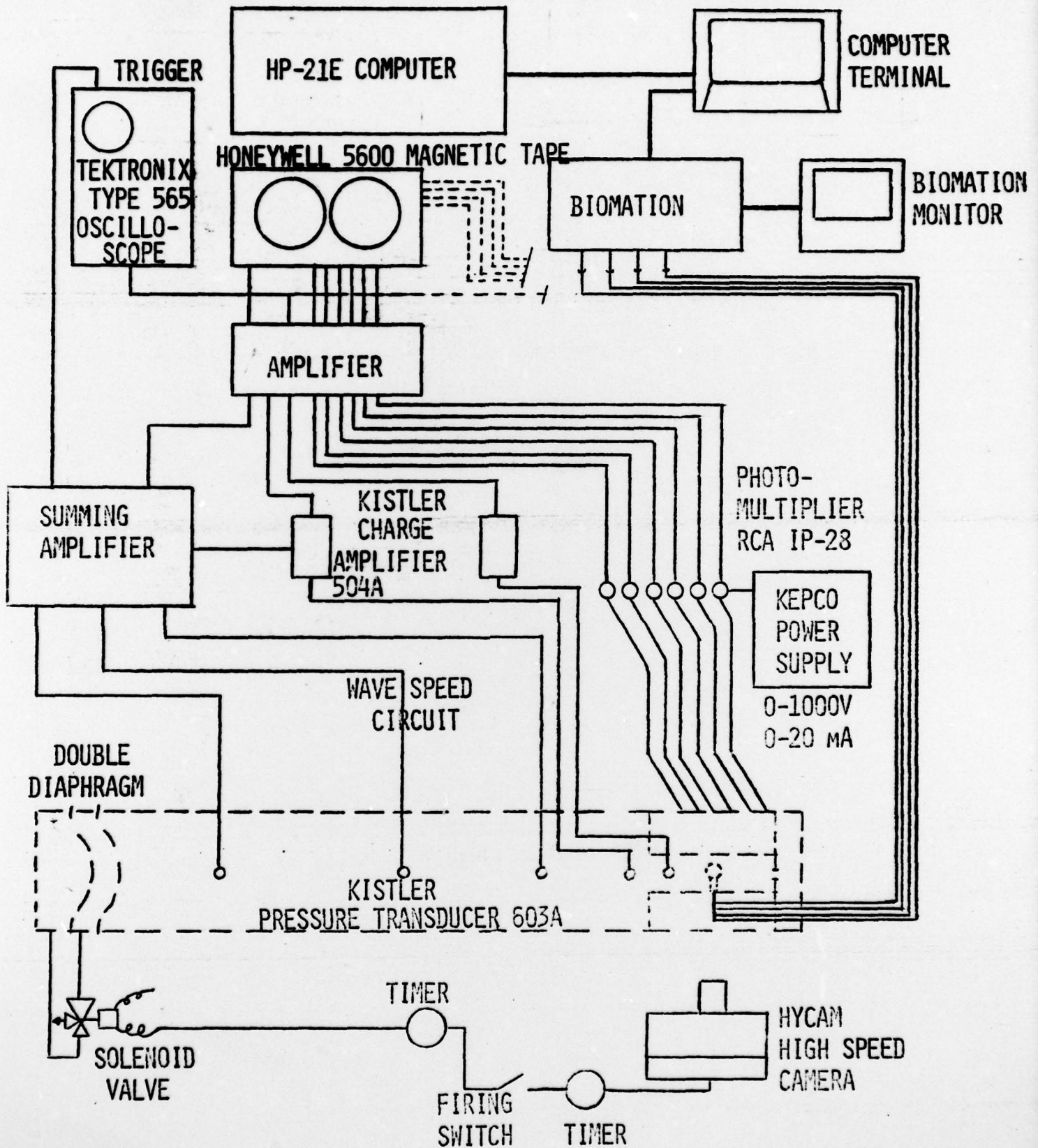
INSTRUMENTATION FOR CONVECTIVE IGNITION EXPERIMENT

Fig. 1   Instrumentation for convective ignition experiment.

MEASURED HEAT FLUXES

PRESSURE: 1.6 MPa
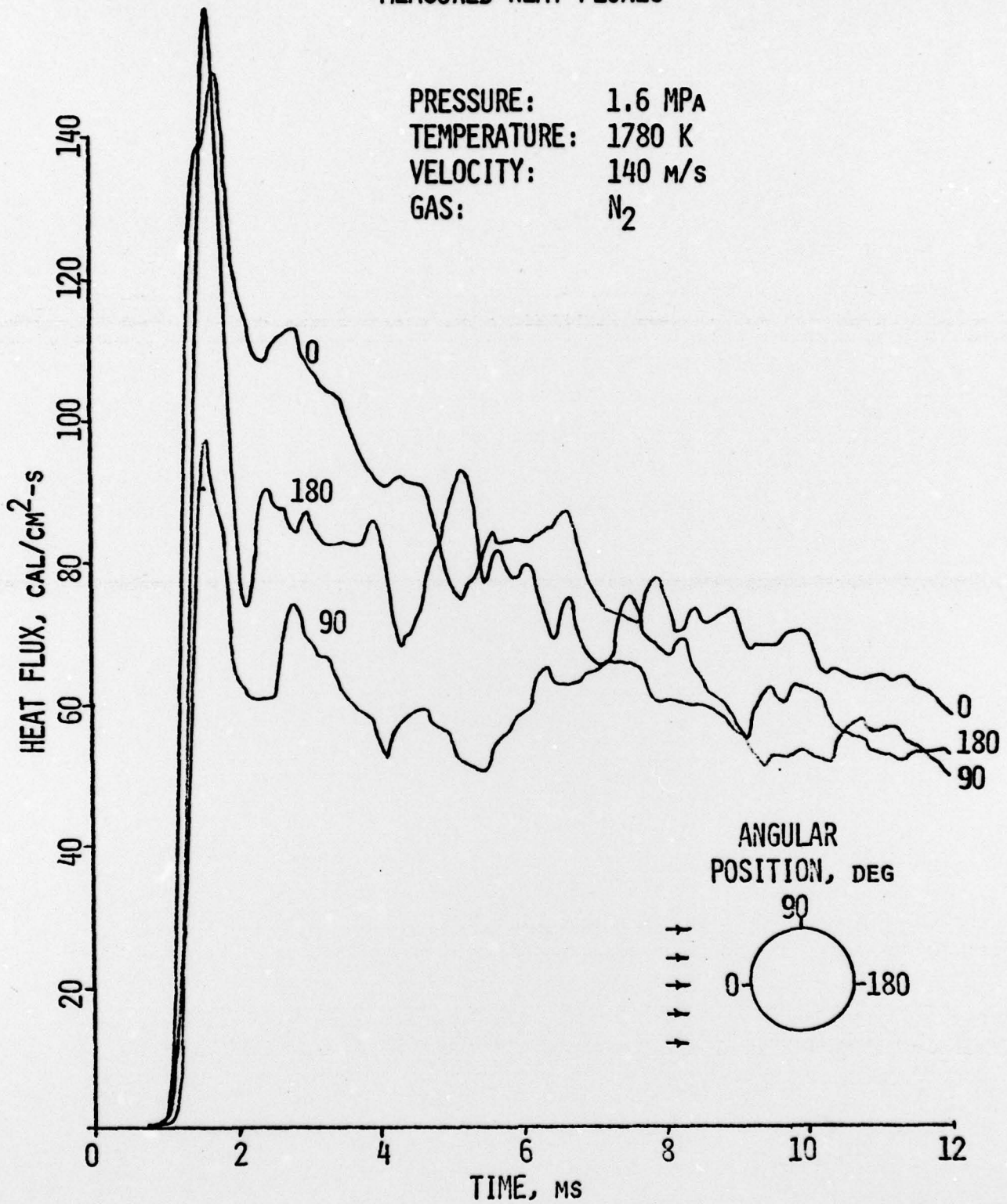TEMPERATURE: 1780 K
VELOCITY: 140 m/s
GAS: N_2

Fig. 2   Heat fluxes measured by three thin film
gages on 7 mm cylinder.

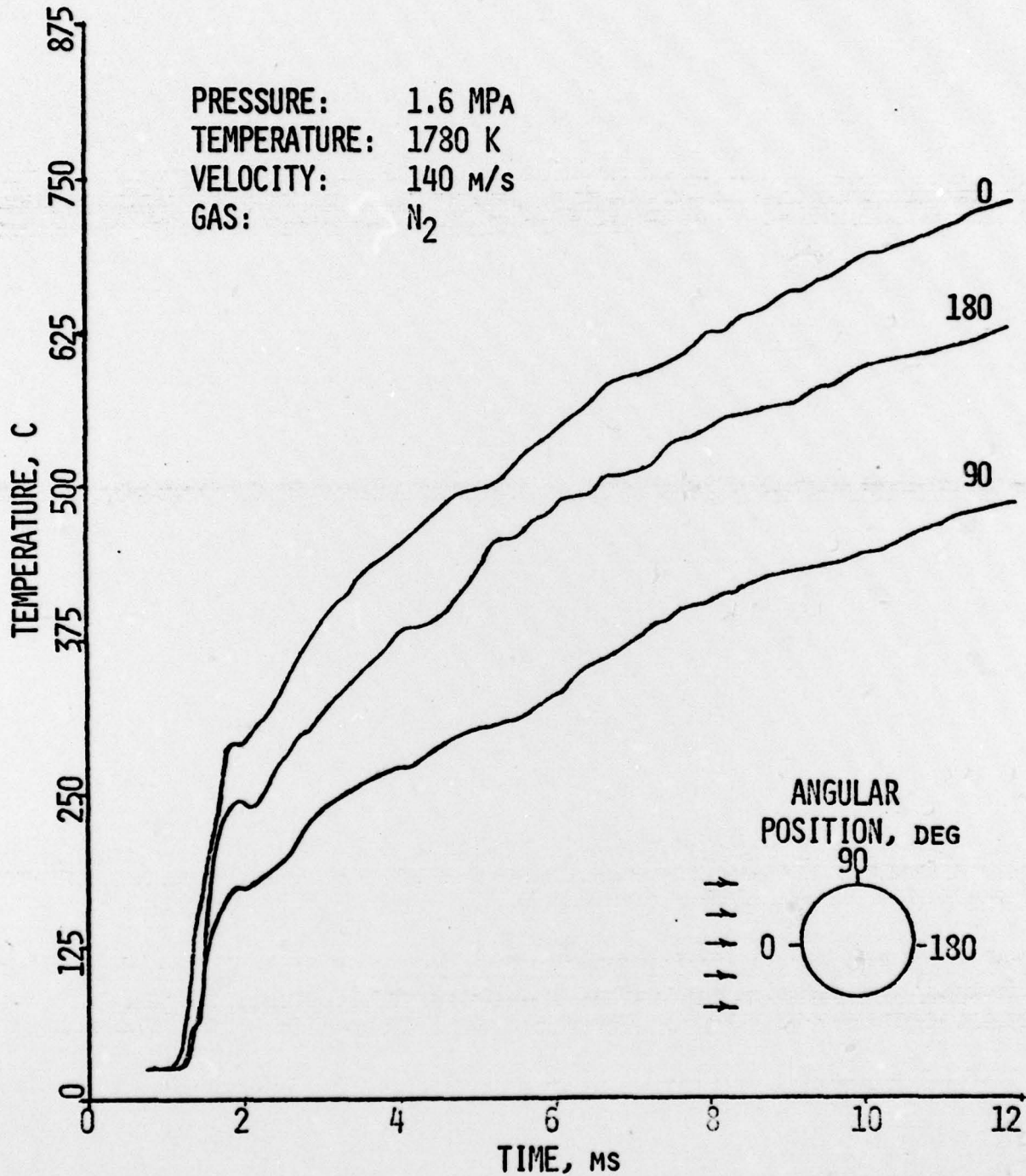# CALCULATED SURFACE TEMPERATURES CORRESPONDING TO MEASURED HEAT FLUXES

PRESSURE: 1.6 MPa
TEMPERATURE: 1780 K
VELOCITY: 140 m/s
GAS: N_2

Fig. 3   Calculated propellant surface temperatures corresponding to measured heat fluxes.
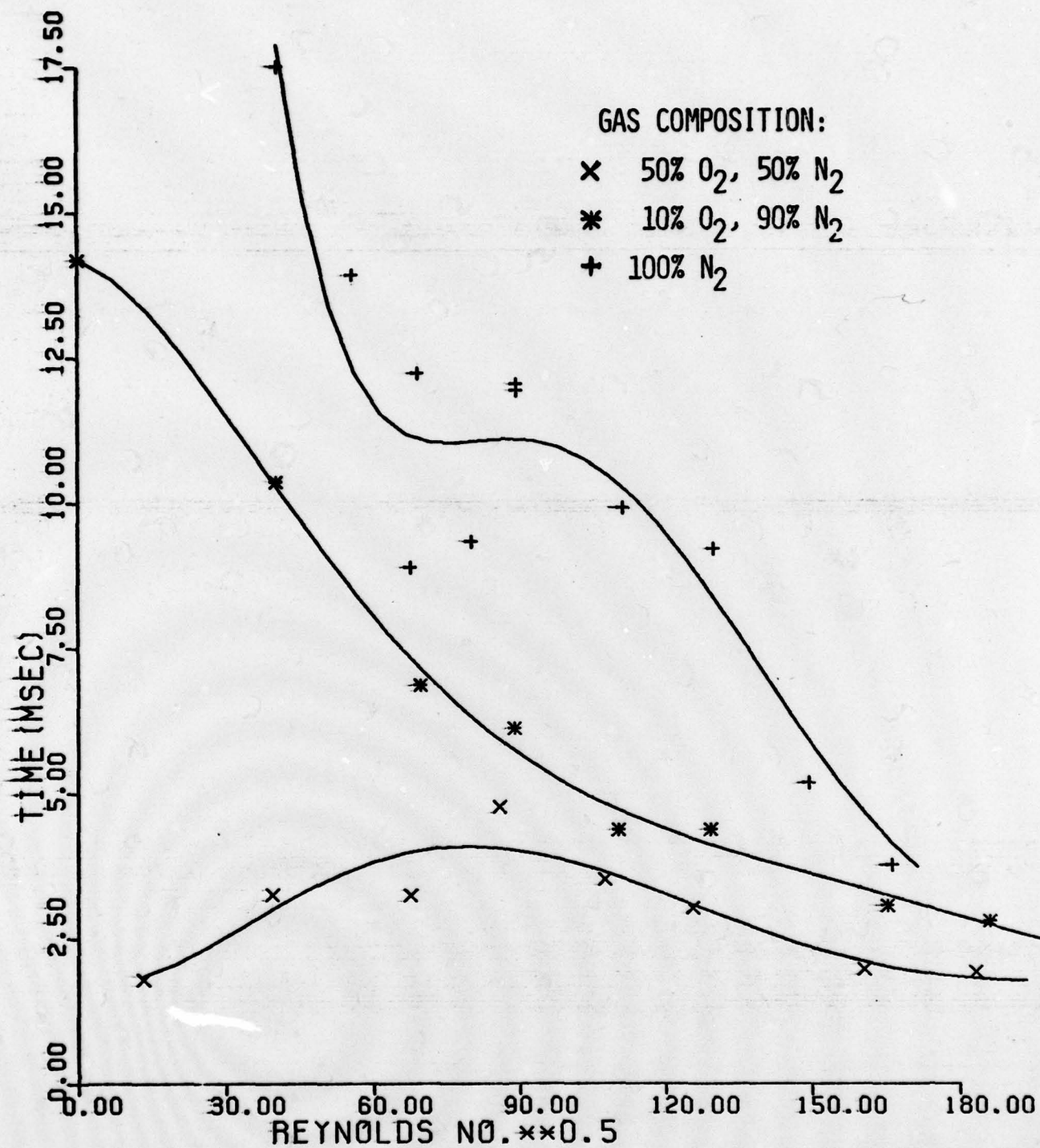
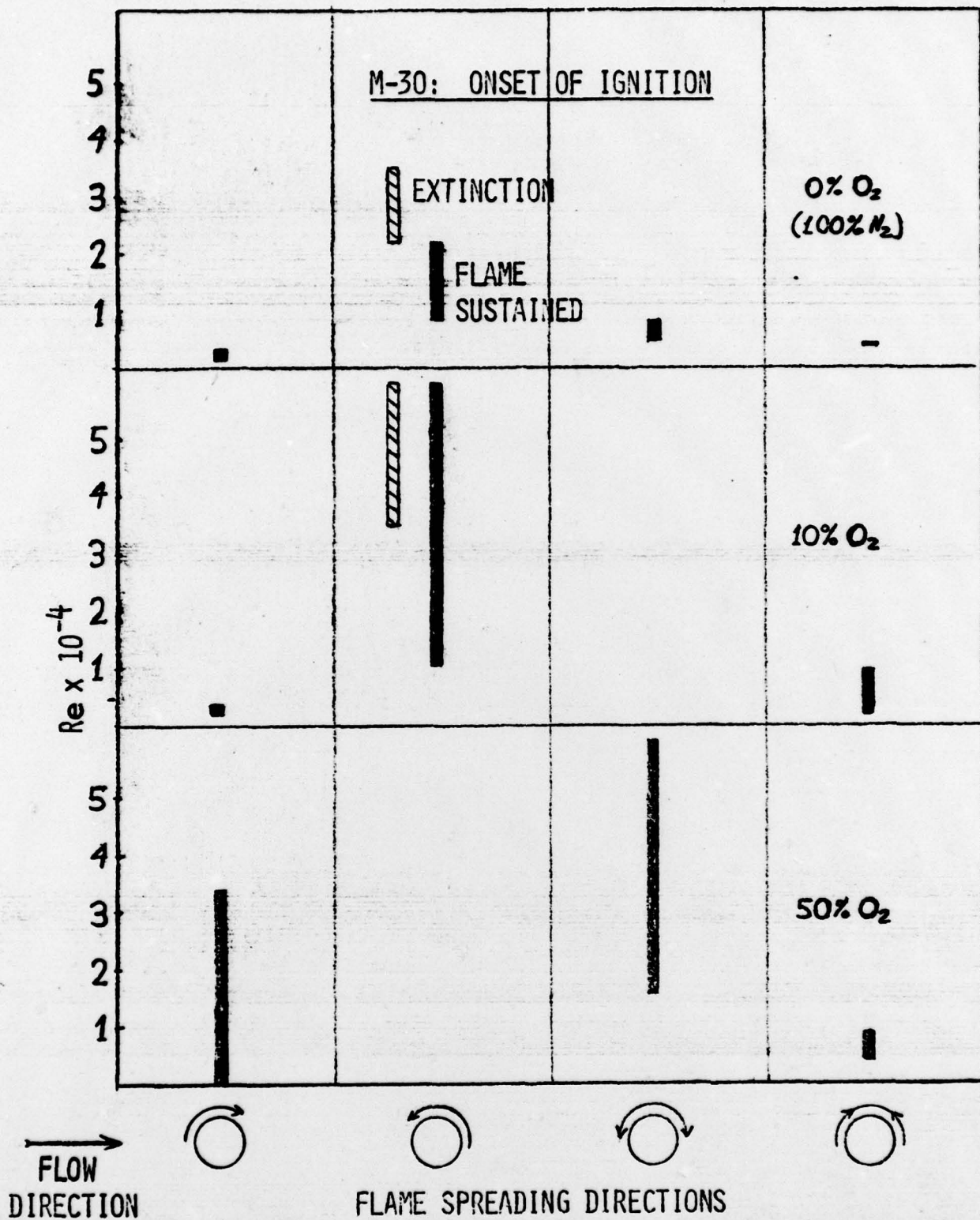**Fig. 4   Measured ignition times for M 30 propellant.**

Fig. 5   Flame spreading characteristics of M30 as a function of oxygen concentration and Reynolds number.
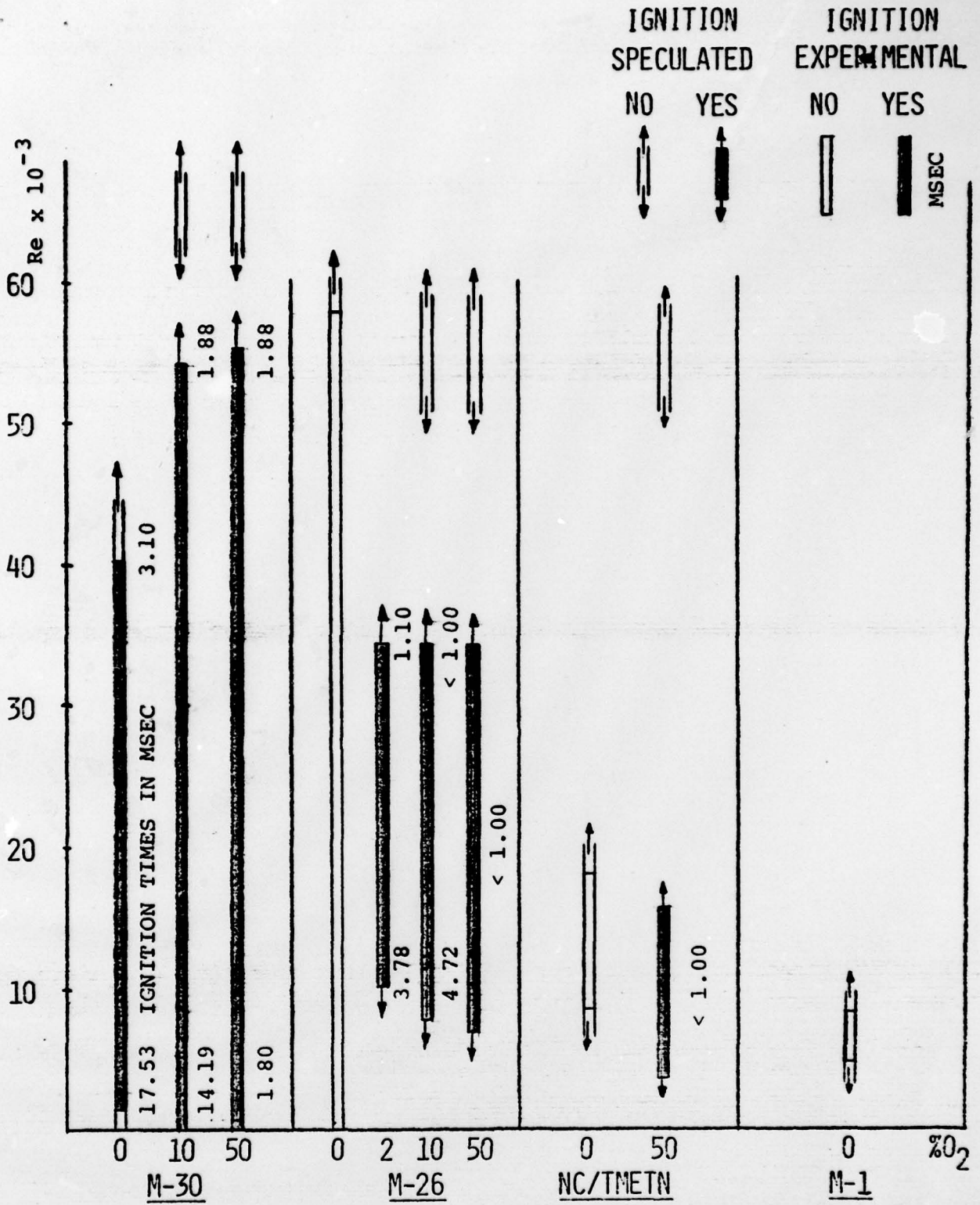
Fig. 6   Ignition trends for several nitro-
cellulose based propellants.

CONVECTIVE IGNITION

t = 0 ms
ARRIVAL OF SHOCK WAVE

t = 1.25 ms
SUSTAINED FLAME ESTABLISHED

t = 0.25 ms
GASIFICATION AND FIRST
EVIDENCE OF IGNITION AT 90°

t = 1.50 ms
FLAME ESTABLISHED AT
LEADING EDGE

t = 0.50 ms
TRANSIENT FLAME DEVELOPMENT
AT 90° (VAPORS ORIGINATED
AT FRONT SECTION)

t = 1.75 ms
FLAME ESTABLISHED AT
LEADING EDGE

t = 0.75 ms
VAPORS BURNED OUT

t > 5 ms
BURNING IN WAKE

t = 1.00 ms
FLAME REDEVELOPING

t > 5 ms
BURNING IN WAKE

Fig. 7   Photographs showing convective ignition events
(M26 Propellant, 1.63 MPa, 1740 K, 140 m/s,
50% N_2 & 50% O_2,   Re = 55,000).

BOUNDARY LAYER

REGION (B) SEPARATION FLOW ZONE

REGION (A) STAGNATION FLOW ZONE

U_e

REGION (c)

REAR BODY FLOW

U_∞
T_∞
P_∞
$Y_{OX\infty}$

DETAILS OF SEPARATION REGION

U_B

Y_{FB}

Y_{FS} Y_{OXS}
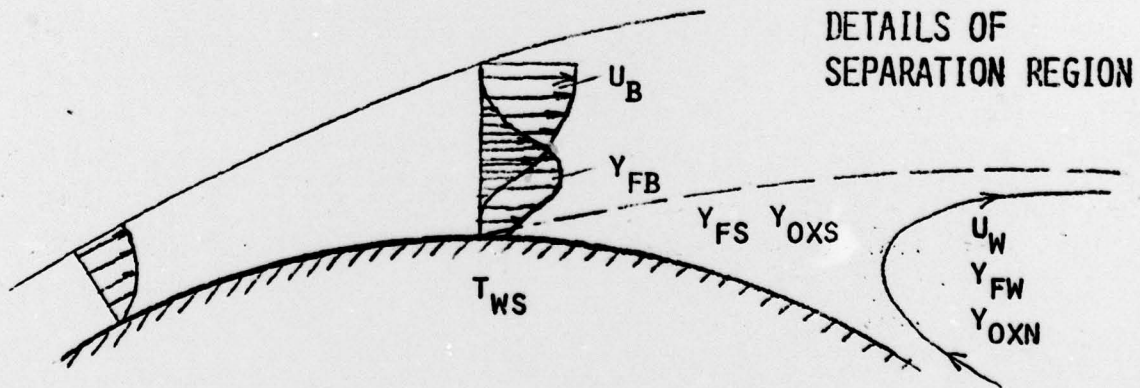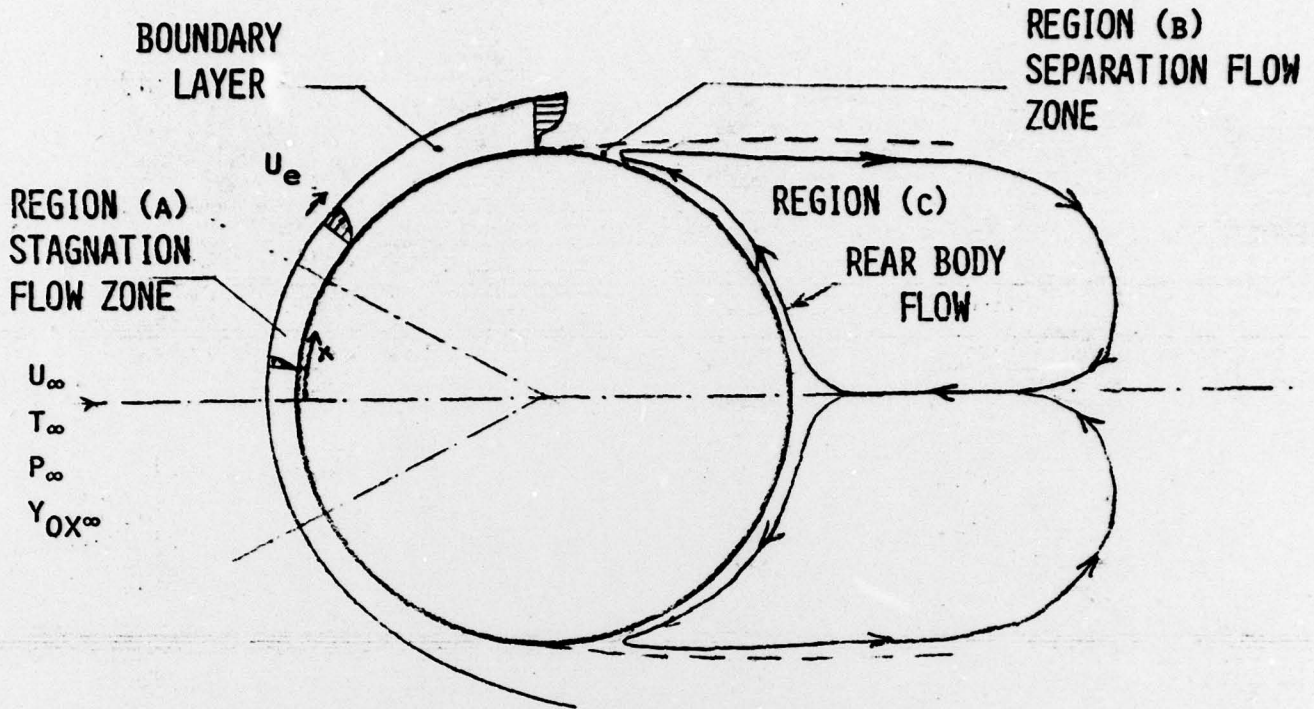
U_W
Y_{FW}
Y_{OXN}

T_{WS}

Fig. 8   Main ignition regions of propellant cylinder in crossflow.

REFERENCES

1. Warren C. Strahle, "A Transient Problem on the Evaporation of a Reactive Fuel," Combustion Science and Technology, Vol. 1 1969, pp. 25-33.

2. R. K. Kumar and C. E. Hermance, "Fundamental Processes in Solid Propellant Ignition," AFOSR Final Scientific Report AFOSR-TR-71-1968.

3. John W. Mitchell, "Base Heat Transfer in Two-Dimensional Subsonic Fully Separated Flows," Transactions of the ASME Journal of Heat Transfer, November 1971, pp. 342-348.

4. P. S. Virk, "Heat Transfer from the Rear of a Cylinder in Transverse Flow," Transactions of the ASME Journal of Heat Transfer, February 1970, pp. 206-207.

5. Hiroshi Matsui, et al., "Heat Transfer Phenomena in Wake Flow of Cylinder," Fourth International Heat Conference in Paris 2, FC5.9, 1970.